

Fermion soliton stars and black holes

T. D. Lee and Y. Pang

Columbia University, New York, New York 10027

(Received 28 October 1986)

Explicit solutions of fermion soliton stars and fermion black holes are given. The former has no horizon and the latter does. The soliton stars are cold, stable, and coherent states of very large mass $M \sim (l_P m)^{-4} m$, with l_P the Planck length, m the mass of the relevant Higgs-type scalar field, and $\hbar=c=1$.

I. INTRODUCTION

This paper extends the analysis of the previous three papers¹⁻³ to fermion soliton stars and fermion black holes. These objects are supposed to carry zero (total) electric charge, and the fermions are representatives of either quarks, or any other spin- $\frac{1}{2}$ particles.

We discuss first the fermion soliton star. The necessary and sufficient conditions for such a configuration are (i) the conservation of the fermion number N and (ii) the existence of nontopological soliton solutions,^{4,5} in the absence of the gravitational field. It is the latter condition that distinguishes a soliton star from a neutron star, or a white dwarf.

In order to satisfy (ii), we assume the existence of a Hermitian scalar field σ , in addition to the fermion field ψ and the gravitational field $g_{\mu\nu}$. The simplest example is when the self-interaction of σ is of the degenerate vacuum form (in units $\hbar=c=1$):

$$U(\sigma) = \frac{1}{2} \mu^2 \sigma^2 \left[1 - \frac{\sigma}{\sigma_0} \right]^2, \quad (1.1)$$

with $\mu = \sigma$ mass. We may assign $\sigma=0$ to the normal vacuum state, and $\sigma = \sigma_0$ to the false (or degenerate) vacuum state. (Theories of this type have been extensively studied in the literature, e.g., in connection with the abnormal nuclear matter,⁶ with the bag model,^{7,8} and with spontaneous T violation.^{9,10}) The interaction between σ and ψ is

$$-f \bar{\psi} \psi \sigma, \quad (1.2)$$

where f is the coupling and $\bar{\psi}$ is the adjoint of ψ , making $\bar{\psi} \psi$ a Lorentz scalar. Let the fermion mass (in the normal vacuum) be m . For simplicity we assume

$$m - f\sigma_0 = 0, \quad (1.3)$$

so that the fermion has a zero effective mass in the false vacuum.

For orientation purposes, we repeat here the qualitative feature of a fermion soliton star already discussed in I. Consider first the example of a nontopological soliton without gravity. The soliton contains an interior in which $\sigma \simeq \sigma_0$, a shell of width $\sim \mu^{-1}$, over which σ changes from σ_0 to 0, and an exterior that is essentially the vacuum. The fermion field ψ is confined to the interior; this produces a kinetic energy E_k :

$$E_k \simeq \frac{1}{2} \left(\frac{3}{2} \right)^{5/3} \pi^{1/3} N^{4/3} / R. \quad (1.4)$$

The shell contains a surface energy

$$E_s = 4\pi s R^2,$$

where s is the surface tension, related to σ_0 and μ by

$$s \simeq \frac{1}{6} \mu \sigma_0^2. \quad (1.5)$$

The radius R can be calculated by minimizing the total energy $E = E_k + E_s$. Setting $\partial E / \partial R = 0$, we have the equipartition

$$E_k = 2E_s. \quad (1.6)$$

Hence, the soliton mass M (which is the minimum of E) can be written as

$$M = 3E_s = 12\pi s R^2, \quad (1.7)$$

the total fermion number is related to R by

$$N \propto R^{9/4}, \quad (1.8)$$

and therefore, for large N ,

$$M \propto N^{8/9}. \quad (1.9)$$

Because the exponent of N is < 1 , when N is large the soliton mass is always less than that of the free particle solution, and that ensures its stability.

Next, we include the gravitational field. For configurations with R much greater than the Schwarzschild radius $2GM$, the effects of gravity can be treated as a perturbation. Gravity becomes important when R becomes of the same order as $2GM$. Hence, the critical mass M_c for the formation of a black hole may be estimated by simply equating R with the Schwarzschild radius

$$R \sim 2GM_c,$$

which leads to, because of (1.7),

$$M_c \sim (48\pi G^2 s)^{-1}. \quad (1.10)$$

Since Newton's constant G is the square of the Planck length $l_P \simeq 10^{-33}$ cm, whereas a typical Higgs-type field σ may have $\sigma_0 \sim \mu$ about, or higher than, 30 GeV (but much less than the Planck mass), we have

$$M_c \sim (l_P \mu)^{-4} \mu \quad (1.11)$$

which is $\sim 10^{15}M_\odot$, with a corresponding radius $R \sim l_p^{-2}\mu^{-3} \sim 10^2$ light years, for $\mu \sim 30$ GeV.

At present, very little is known concerning the nature of the Higgs-type bosons, except that they should be massive, spin 0, and have expectation values which modify the masses of other fields. Thus, M_c for the soliton star could also be much less than the above estimate, depending on the theory.

In Sec. II we give the general formalism of the problem for a spherically symmetric system consisting of ψ , σ , and $g_{\mu\nu}$. The detailed solution of a fermion soliton star is given in Sec. III, and that of a black hole in Sec. IV.

Since the theory has a particle-antiparticle system, we need only give the explicit solution for $N > 0$.

II. GENERAL FORMULATION

In this paper, we consider only the spherically symmetric solutions. The square of the length differential can be written in terms of the spherical coordinates (t, ρ, α, β) as

$$ds^2 = -e^{2u}dt^2 + e^{2\bar{v}}d\rho^2 + \rho^2(d\alpha^2 + \sin^2\alpha d\beta^2) \quad (2.1)$$

or in terms of the isotropic coordinates (t, r, α, β) as

$$ds^2 = -e^{2u}dt^2 + e^{2v}(dr^2 + r^2d\alpha^2 + r^2\sin^2\alpha d\beta^2), \quad (2.2)$$

where α, β are the standard polar and azimuthal angles, and ρ is $(2\pi)^{-1}$ times the circumference (i.e., the length of the great circle) of a sphere, related to r by

$$\rho = re^v. \quad (2.3)$$

The functions u , v , and \bar{v} depend only on r , or, equivalently, only on ρ . As in II and III, it is useful to define

$$\begin{aligned} x &\equiv \dot{u} \equiv ru', \\ y &\equiv 1 + \dot{v} \equiv 1 + rv' = e^{-\bar{v}} = d \ln \rho / d \ln r, \end{aligned} \quad (2.4)$$

where

$$u' = du/dr, \quad v' = dv/dr.$$

Likewise, we introduce

$$\begin{aligned} u'' &= d^2u/dr^2, \quad v'' = d^2v/dr^2, \\ x' &= dx/dr, \quad y' = dy/dr, \\ \dot{x} &= rx', \quad \dot{y} = ry'. \end{aligned} \quad (2.5)$$

A. Thomas-Fermi approximation and the total energy

For the fermion field ψ , we shall adopt the Thomas-Fermi approximation. At each point in space there is a Fermi momentum k_F (observed in the appropriate local frame) which, for the spherically symmetric solution, depends only on ρ , or equivalently only on r . The fermion energy density is given by the familiar expression

$$W = \frac{2}{8\pi^3} \int d^3k n_k \epsilon_k, \quad (2.6)$$

where the factor 2 is due to the spin degeneracy, $\int d^3k = 4\pi \int k^2 dk$, n_k is the Fermi distribution

$$n_k = \theta(k - k_F) = \begin{cases} 1 & \text{if } k < k_F, \\ 0 & \text{if } k > k_F, \end{cases} \quad (2.7)$$

and, on account of (1.2) and (1.3),

$$\epsilon_k = [k^2 + (m - f\sigma)^2]^{1/2}. \quad (2.8)$$

The corresponding fermion number density ν and the nonzero components of the stress tensor T_ν^μ are

$$\nu = \frac{2}{8\pi^3} \int d^3k n_k, \quad (2.9)$$

$$T_i^i = W, \quad (2.10)$$

$$T_r^r = T_\alpha^\alpha = T_\beta^\beta = T_\rho^\rho \equiv -T,$$

where

$$T = \frac{2}{8\pi^3} \int d^3k n_k \frac{k^2}{3\epsilon_k}. \quad (2.11)$$

Consequently, they satisfy the identities

$$T_\mu^\mu = W - 3T = (m - f\sigma)S \quad (2.12)$$

and

$$W - T = \epsilon_F \nu, \quad (2.13)$$

where S is the scalar density $\bar{\psi}\psi$ in the Thomas-Fermi approximation,

$$S = \frac{2}{8\pi^3} \int d^3k n_k \epsilon_k^{-1} (m - f\sigma), \quad (2.14)$$

and ϵ_F is the Fermi energy, related to k_F by

$$\epsilon_F = [k_F^2 + (m - f\sigma)^2]^{1/2}. \quad (2.15)$$

The total fermion number N and the total fermion energy $E(f)$ are given by

$$N = 4\pi \int e^{\bar{v}} \rho^2 d\rho \nu = 4\pi \int e^{3v} r^2 dr \nu \quad (2.16)$$

and

$$E(f) = 4\pi \int e^{u+\bar{v}} \rho^2 d\rho W = 4\pi \int e^{u+3v} r^2 dr W. \quad (2.17)$$

The total energy of the system consists of, besides $E(f)$, also the gravitational energy $E(g)$ and the σ field energy $E(\sigma)$:

$$E = E(f) + E(g) + E(\sigma), \quad (2.18)$$

where

$$\begin{aligned} E(g) = -(2G)^{-1} \int e^u &\left[e^{\bar{v}} - 2 \left[1 + \rho \frac{du}{d\rho} \right] \right. \\ &\left. + e^{-\bar{v}} \left[1 + 2\rho \frac{du}{d\rho} \right] \right] d\rho, \end{aligned} \quad (2.19)$$

or, equivalently,

$$E(g) = -(2G)^{-1} \int e^{u+v} (2u'v' + v'^2) r^2 dr. \quad (2.20)$$

For the lowest-energy state, σ is time independent; there-

fore

$$\begin{aligned} E(\sigma) &= 4\pi \int e^{u+\bar{v}}(U+V)\rho^2 d\rho \\ &= 4\pi \int e^{u+3v}(U+V)r^2 dr, \end{aligned} \quad (2.21)$$

where $U(\sigma)$ is given by (1.1) and

$$V = \frac{1}{2} e^{-2\bar{v}} \left[\frac{d\sigma}{d\rho} \right]^2 = \frac{1}{2} e^{-2v} \left[\frac{d\sigma}{dr} \right]^2. \quad (2.22)$$

While almost all the Thomas-Fermi formulas in this and the next sections are well known, a derivation is given in the Appendix.

B. Variational principles and the basic equations

Regard the total energy E , given by (2.18), as a functional of k_F , σ , u , and v (or equivalently \bar{v}). The basic equations can be obtained by taking the extremity of E of a fixed N ; i.e.,

$$\delta E - \omega_F \delta N = 0, \quad (2.23)$$

where ω_F is the Lagrange multiplier. As we shall see, this leads to the Einstein equations plus those of k_F and σ . Their solution gives the soliton mass

$$M = E = E(f) + E(g) + E(\sigma). \quad (2.24)$$

Let L be the corresponding Lagrangian in the Thomas-Fermi approximation:

$$L \equiv N\omega_F - E. \quad (2.25)$$

From (2.23), N can be expressed in terms of ω_F and the other variables k_F, σ, u, v . Substituting that expression into (2.25), we may regard $L = L(k_F, \sigma, u, v, \omega_F)$. Equation (2.23) is identical to taking the extremity of L at a fixed ω_F ; i.e.,

$$\delta L - N\delta\omega_F = 0,$$

with N now appearing as a Lagrange multiplier.

Let $\mathcal{R}_{\mu\nu}$ be the Ricci tensor and $\mathcal{R} = g^{\mu\nu}\mathcal{R}_{\mu\nu}$ the scalar curvature. Einstein's equations relate

$$G_{\mu\nu} = \mathcal{R}_{\mu\nu} - \frac{1}{2}g_{\mu\nu}\mathcal{R}$$

to the matter tensor: in the spherical coordinates (t, ρ, α, β) we have

$$\begin{aligned} \rho^2 G_t^t &= e^{-2\bar{v}} - 1 - 2e^{-2\bar{v}}\rho \frac{d\bar{v}}{d\rho} \\ &= -8\pi G\rho^2(W+V+U), \end{aligned} \quad (2.26)$$

$$\begin{aligned} \rho^2 G_\rho^\rho &= e^{-2\bar{v}} - 1 + 2e^{-2\bar{v}}\rho \frac{du}{d\rho} \\ &= 8\pi G\rho^2(T+V-U), \end{aligned} \quad (2.27)$$

and

$$\begin{aligned} \rho^2 G_\alpha^\alpha &= e^{-2\bar{v}} \left[\rho^2 \frac{d^2 u}{d\rho^2} + \left(1 + \rho \frac{du}{d\rho} \right) \rho \frac{d}{d\rho} (u - \bar{v}) \right] \\ &= 8\pi G\rho^2(T - V - U); \end{aligned} \quad (2.28)$$

the last one is identical to that for $\rho^2 G_\beta^\beta$. In the isotropic coordinates (t, r, α, β) , these equations become

$$2v'' + v'^2 + \frac{4}{r}v' = -8\pi G e^{2v}(W+V+U), \quad (2.26')$$

$$2u'v' + v'^2 + \frac{2}{r}(u'+v') = 8\pi G e^{2v}(T+V-U), \quad (2.27')$$

and

$$u'' + v'' + u'^2 + \frac{1}{r}(u'+v') = 8\pi G e^{2v}(T - V - U), \quad (2.28')$$

or, in terms of x and y ,

$$2\dot{y} + y^2 - 1 = -8\pi G r^2 e^{2v}(W+V+U), \quad (2.29)$$

$$2xy + y^2 - 1 = 8\pi G r^2 e^{2v}(T+V-U), \quad (2.30)$$

and

$$\dot{x} + \dot{y} + x^2 = 8\pi G r^2 e^{2v}(T - V - U), \quad (2.31)$$

where W , T , V , and U are given by (2.6), (2.11), (2.22), and (1.1).

The fermion distribution, characterized by the Fermi momentum k_F , is given by

$$[k_F^2 + (m - f\sigma)^2]^{1/2} e^u = \epsilon_F e^u = \omega_F = \text{const} \quad (2.32)$$

and the σ field equation is

$$e^{-2\bar{v}} \left[\frac{d^2 \sigma}{d\rho^2} + \left(\frac{2}{\rho} + \frac{du}{d\rho} - \frac{d\bar{v}}{d\rho} \right) \frac{d\sigma}{d\rho} \right] + fS - \frac{dU}{d\sigma} = 0, \quad (2.33)$$

or, equivalently,

$$e^{-2v} \left[\sigma'' + \left(u' + v' + \frac{2}{r} \right) \sigma' \right] + fS - \frac{dU}{d\sigma} = 0 \quad (2.33')$$

with $\sigma' = d\sigma/dr$, $\sigma'' = d^2\sigma/dr^2$, and S given by (2.14). These five equations, (2.26)–(2.28), (2.32), and (2.33) satisfy one identity, given by $G_{\nu;\mu}^\mu = 0$:

$$\frac{du}{d\rho} G_t^t - \left[\frac{2}{\rho} + \frac{du}{d\rho} + \frac{d}{d\rho} \right] G_\rho^\rho + \frac{2}{\rho} G_\alpha^\alpha = 0 \quad (2.34)$$

or, equivalently,

$$u' G_t^t - \left[\frac{2}{r} + u' + 2v' + \frac{d}{dr} \right] G_r^r + 2 \left[\frac{1}{r} + v' \right] G_\alpha^\alpha = 0. \quad (2.34')$$

Outside the soliton radius R , the Fermi momentum k_F is zero; therefore, from (2.33) we see that

$$\sigma = O(e^{-\mu\rho}) \text{ as } \rho \rightarrow \infty.$$

Correspondingly, in the spherical coordinates, as $\rho \rightarrow \infty$ we have the Schwarzschild solution

$$\begin{aligned} e^u &\sim \left[1 - \frac{4a}{\rho} \right]^{1/2}, \\ e^{\bar{v}} &\sim \left[1 - \frac{4a}{\rho} \right]^{-1/2}, \end{aligned} \quad (2.35)$$

or, equivalently, in the isotropic coordinates, as $r \rightarrow \infty$

$$\begin{aligned} e^u &\sim \frac{r-a}{r+a}, \\ e^v &\sim \left(\frac{r+a}{r} \right)^2, \end{aligned} \quad (2.36)$$

where

$$a = \frac{1}{2}GM. \quad (2.37)$$

C. Soliton mass

The soliton mass M is defined by (2.24). As is well known,¹¹ the same M can also be derived by using the asymptotic behavior of the metric $g_{\rho\rho} = e^{2\bar{v}}$ or $g_{tt} = -e^{2u}$ at $\rho = \infty$:

$$M = \lim_{\rho \rightarrow \infty} \rho \bar{v} / G \quad (2.38)$$

or

$$M = - \lim_{\rho \rightarrow \infty} \rho u / G.$$

These formulas can be established by using (2.26); we find

$$\frac{d}{d\rho} [\rho e^u (1 - e^{-\bar{v}})] = G \frac{d}{d\rho} [E(g) + E(f) + E(\sigma)], \quad (2.39)$$

where, because of (2.17) and (2.19)–(2.21),

$$\begin{aligned} \frac{d}{d\rho} E(g) &\equiv (2G)^{-1} e^u \left[-e^{\bar{v}} + 2 \left[1 + \rho \frac{du}{d\rho} \right] \right. \\ &\quad \left. - e^{-\bar{v}} \left[1 + 2\rho \frac{d\bar{v}}{d\rho} \right] \right] \end{aligned}$$

and

$$\frac{d}{d\rho} [E(f) + E(\sigma)] \equiv 4\pi \rho^2 e^{u+\bar{v}} (W + V + U).$$

The integration of (2.39) gives the top equation in (2.38) directly. The Schwarzschild form (2.35) gives then the second equation in (2.38).

There are many alternative formulas for M : (2.26) and (2.26') can also be written as

$$\frac{d}{d\rho} [\rho(1 - e^{-2\bar{v}})] = 8\pi G \rho^2 (W + V + U) \quad (2.40)$$

and

$$\frac{d}{dr} \left[e^{v/2} r^2 \frac{dv}{dr} \right] = -4\pi G r^2 e^{5v/2} (W + V + U). \quad (2.41)$$

Upon integration and using the Schwarzschild solution at ∞ , we obtain

$$M = 4\pi \int_0^\infty (W + V + U) \rho^2 d\rho \quad (2.42)$$

and

$$M = 4\pi \int_0^\infty (W + V + U) e^{5v/2} r^2 dr. \quad (2.43)$$

Either expression establishes the positivity of M . In addition, from (2.40) and $\bar{v} = 0$ at ∞ , it follows that (for soliton stars)

$$0 \leq y = e^{-\bar{v}} \leq 1. \quad (2.44)$$

By taking the combination $G_\alpha^\alpha + \frac{1}{2}(G_\rho^\rho - G_t^t)$, we have

$$\frac{d}{d\rho} \left[\rho^2 e^{u-\bar{v}} \frac{du}{d\rho} \right] = 8\pi G \rho^2 e^{u+\bar{v}} \left(\frac{3}{2}T + \frac{1}{2}W - U \right), \quad (2.45)$$

which leads to still another formula for M :

$$\begin{aligned} M &= 8\pi \int_0^\infty \left(\frac{3}{2}T + \frac{1}{2}W - U \right) e^{u+\bar{v}} \rho^2 d\rho \\ &= 8\pi \int_0^\infty \left(\frac{3}{2}T + \frac{1}{2}W - U \right) e^{u+3v} r^2 dr. \end{aligned} \quad (2.46)$$

Another relation can be obtained by considering the difference $G_\rho^\rho - G_t^t$; this gives

$$\frac{d}{d\rho} (u + \bar{v}) = 4\pi G \rho e^{2\bar{v}} (T + W + 2V) \quad (2.47)$$

and is always positive. Because $u + \bar{v} = 0$ at ∞ , we have (for soliton stars)

$$u + \bar{v} < 0 \quad (2.48)$$

at all finite ρ .

D. Behavior near the origin

From (2.26), (2.27), (2.32), and (2.33), we see that, as $\rho \rightarrow 0$,

$$\begin{aligned} u &= u(0) + O(\rho^2), \\ \bar{v} &= O(\rho^2), \\ \sigma &= \sigma(0) + O(\rho^2), \\ k_F &= k_F(0) + O(\rho^2). \end{aligned} \quad (2.49)$$

These imply that in the isotropic coordinates, as $r \rightarrow 0$ the variables x and y , defined by (2.4), are of the form

$$x = \frac{1}{2}ar^2 + O(r^4) \quad (2.50)$$

and

$$y = 1 + \frac{1}{2}br^2 + O(r^4),$$

where a and b are constants. By using (2.29)–(2.31), we find

$$\left[\frac{dx}{dy} \right]_0 \equiv \frac{a}{b} = \frac{2U(0) - 3T(0) - W(0)}{U(0) + W(0)}, \quad (2.51)$$

where $U(0)$, $T(0)$, and $W(0)$ are the values of U , T , and W at $r = 0$. [Note that $V(0) = 0$ because of (2.49).]

Equation (2.51) is valid for any $U(\sigma)$. In our problem, as we shall see, for $U(0)$ given by (1.1) with σ_0 satisfying (1.3), $\sigma = \sigma_0$ and $T = \frac{1}{3}W$ in the interior; consequently,

$$\left[\frac{dx}{dy} \right]_0 = -2. \quad (2.52)$$

III. SOLITON STAR

A. Interior: $\rho < R + O(\mu^{-1})$

For U given by (1.1), its derivative is

$$\frac{dU}{d\sigma} = \mu^2(\sigma - \sigma_0)(2\sigma - \sigma_0)\sigma/\sigma_0^2. \tag{3.1}$$

In the interior, we set

$$\sigma = \sigma_0; \tag{3.2}$$

therefore, it follows from (1.3), (2.14), and (3.1) that

$$\frac{dU}{d\sigma} = (m - f\sigma) = S = 0. \tag{3.3}$$

The field equation of σ , (2.33), is satisfied. For the same reason,

$$V = U = 0 \tag{3.4}$$

and

$$3T = W = \frac{k_F^4}{4\pi^2}, \tag{3.5}$$

where, because of (2.32) and (3.3),

$$k_F e^u = \omega_F = \text{const}. \tag{3.6}$$

Equations (2.26) and (2.27) become

$$2\rho \frac{d\bar{v}}{d\rho} = \left[\frac{2}{\pi} G \omega_F^4 e^{-4u} \rho^2 - 1 \right] e^{2\bar{v}} + 1, \tag{3.7}$$

$$2\rho \frac{d\bar{u}}{d\rho} = \left[\frac{2}{3\pi} G \omega_F^4 e^{-4u} \rho^2 + 1 \right] e^{2\bar{v}-1}.$$

Because of the boundary condition (2.35) at ∞ , the above equations (3.2)–(3.7) are applicable only in the interior region.

In order to have the Schwarzschild solution outside the star when $\rho > R + O(\mu^{-1})$, there is a transition region $\rho = R + O(\mu^{-1})$ in which σ changes from σ_0 to 0. Away from the transition region, the σ field goes to zero exponentially in the outside; in the inside σ goes to σ_0 , but also exponentially [cf. (3.35) below]:

$$\sigma \sim \sigma_0 \exp(-\mu |\rho - R|) \text{ (outside)}$$

and
$$\sigma - \sigma_0 \sim \sigma_0 \exp(-\mu |\rho - R|) \text{ (inside)}. \tag{3.8}$$

From the estimate (1.7)–(1.11), for M of the same order as M_c , given by (1.10), $\sigma_0 \sim \mu$ of $e^{-u} \sim 1$, we note that

$$R \sim (G\mu^3)^{-1}, \quad M \sim (G^2\mu^3)^{-1}, \tag{3.9}$$

$$N \sim (G\mu^2)^{-9/4}, \quad \omega_F \sim G^{1/4} \mu^{3/2}.$$

Define

$$\lambda \equiv 4\sigma_0(\pi G/3)^{1/2}, \tag{3.10}$$

which for $\sigma_0 \sim 30$ GeV is very small, $\sim 10^{-17}$. [The seemingly complicated factor $4(\pi/3)^{1/2}$ is chosen to make (3.32) and (3.41) below have essentially the same form as in III.] The relevant small parameter is the amplitude

(3.8), away from $\rho = R$; for $\sigma_0 \sim \mu \sim 30$ GeV and $|\rho - R|$ of the same order as R , it is extremely small, of the order of

$$\exp(-\lambda^{-2}) \sim \exp(-10^{34}). \tag{3.11}$$

Thus, the approximation $\sigma = \sigma_0$ in the interior is a reliable one.

Introducing

$$\bar{\rho} \equiv \lambda^2 \mu \rho \tag{3.12}$$

and

$$e^{-\bar{u}} \equiv \left[\frac{3}{8\pi^2} \right]^{1/4} \frac{\omega_F}{(\lambda\mu\sigma_0)^{1/2}} e^{-u},$$

we can rewrite (3.7) as

$$2\bar{\rho} \frac{d\bar{v}}{d\bar{\rho}} = (e^{-4\bar{u}} \bar{\rho}^2 - 1) e^{2\bar{v}} + 1 \tag{3.13}$$

and

$$2\bar{\rho} \frac{d\bar{u}}{d\bar{\rho}} = \left(\frac{1}{3} e^{-4\bar{u}} \bar{\rho}^2 + 1 \right) e^{2\bar{v}} - 1.$$

When $\bar{\rho} \rightarrow 0$, these equations determine

$$\bar{u} = \bar{u}(0) + \frac{1}{6} e^{-4\bar{u}(0)} \bar{\rho}^2 + O(\bar{\rho}^4) \tag{3.14}$$

and

$$\bar{v} = \frac{1}{6} e^{-4\bar{u}(0)} \bar{\rho}^2 + O(\bar{\rho}^4).$$

The interior solution can be obtained by first assigning at $\bar{\rho} = 0$ an initial value

$$e^{-\bar{u}(0)} = \left[\frac{3}{8\pi^2} \right]^{1/4} \frac{\omega_F}{(\lambda\mu\sigma_0)^{1/2}} e^{-u(0)}, \tag{3.15}$$

and then integrating (3.13) numerically from $\rho = 0$ to R ; i.e., from $\bar{\rho} = 0$ to

$$\bar{\rho} = \bar{\rho}_{\text{in}} \equiv \lambda^2 \mu R. \tag{3.16}$$

From the estimates (3.9), we see that $\bar{\rho}$, \bar{u} , u , and \bar{v} are all ~ 1 .

B. (x, y) trajectory

It is convenient to express the solution in terms of the variables x and y , introduced in (2.4). For the interior solution, we may substitute (3.4) and (3.5) into (2.29)–(2.31) and eliminate W between them. The result is, for $\rho < R$,

$$\dot{x} = 5xy + 3y^2 - x^2 - 3, \tag{3.17}$$

$$\dot{y} = -3xy - 2y^2 + 2,$$

and

$$\frac{dy}{dx} = \frac{-3xy - 2y^2 + 2}{5xy + 3y^2 - x^2 - 3}. \tag{3.18}$$

It is convenient to think of

$$\tau \equiv \ln r \tag{3.19}$$

as a fictitious time, $x(\tau)$ and $y(\tau)$ as the trajectory of a “particle,” and $\dot{x}=dx/d\tau$ and $\dot{y}=dy/d\tau$ as its velocity components. Each solution describes a trajectory in the (x,y) plane. As $\bar{\rho}\rightarrow 0$ (therefore $r\rightarrow 0$ and $\tau\rightarrow -\infty$), it follows from (3.14) that

$$x = \frac{1}{3}e^{-4\bar{u}(0)}\bar{\rho}^2 + O(\bar{\rho}^4)$$

and

$$(3.20)$$

$$y = 1 - \frac{1}{6}e^{-4\bar{u}(0)}\bar{\rho}^2 + O(\bar{\rho}^4).$$

There are two critical points of (3.18), defined by $\dot{x}=\dot{y}=0$:

$$(i) \quad x=0, \quad y=1$$

and

$$(3.21)$$

$$(ii) \quad x = \frac{1}{\sqrt{7}}, \quad y = \frac{2}{\sqrt{7}}.$$

From (3.20), we see that at $\rho=0$, the trajectory begins at (i), with an initial slope

$$\left(\frac{dy}{dx}\right)_0 = -\frac{1}{2}, \quad (3.22)$$

in agreement with (2.52). When ρ increases from 0 to R , the interior solution in the (x,y) plane moves along a universal trajectory, called I_F , with the subscript F denoting the fermion case; I_F is completely determined by the first-order differential equation (3.18) with the initial condition (3.22).

In Fig. 1 the dashed curve is the Schwarzschild hyperbola, and the solid curve is I_F . We see that as $\rho\rightarrow\infty$ (therefore r and $\tau=\ln r$ also $\rightarrow\infty$), I_F spirals indefinitely towards the point (ii), $x=1/\sqrt{7}$ and $y=2/\sqrt{7}$. This can be understood by expanding the solution near (ii):

$$x = \frac{1}{\sqrt{7}} + \xi \quad \text{and} \quad y = \frac{2}{\sqrt{7}} + \eta. \quad (3.23)$$

Treating ξ and η as infinitesimals, we can write (3.17) as

$$\frac{d}{d\tau} \begin{pmatrix} \xi \\ \eta \end{pmatrix} = \mathcal{M} \begin{pmatrix} \xi \\ \eta \end{pmatrix}, \quad (3.24)$$

where

$$\mathcal{M} = 7^{-1/2} \begin{pmatrix} 8 & 17 \\ -6 & -11 \end{pmatrix}.$$

The eigenvalues of \mathcal{M} are

$$\frac{1}{2}(-3 \pm i\sqrt{47})/\sqrt{7} \quad (3.25)$$

which shows that as $\tau=\ln r\rightarrow\infty$, the trajectory oscillates indefinitely, with an exponentially decreasing amplitude for ξ and η .

The actual solution depends on the initial value $e^{-\bar{u}(0)}$. By solving (3.13), and using $x=y\bar{\rho}d\bar{u}/d\bar{\rho}$ and $y=e^{-\bar{v}}$ we obtain $x=x(\bar{\rho})$ and $y=y(\bar{\rho})$. Each solution follows the universal trajectory I_F up to a point, called “in” (denoting the inner face of the surface) on I_F , with

$$x = x_{\text{in}} \quad \text{and} \quad y = y_{\text{in}}. \quad (3.26)$$

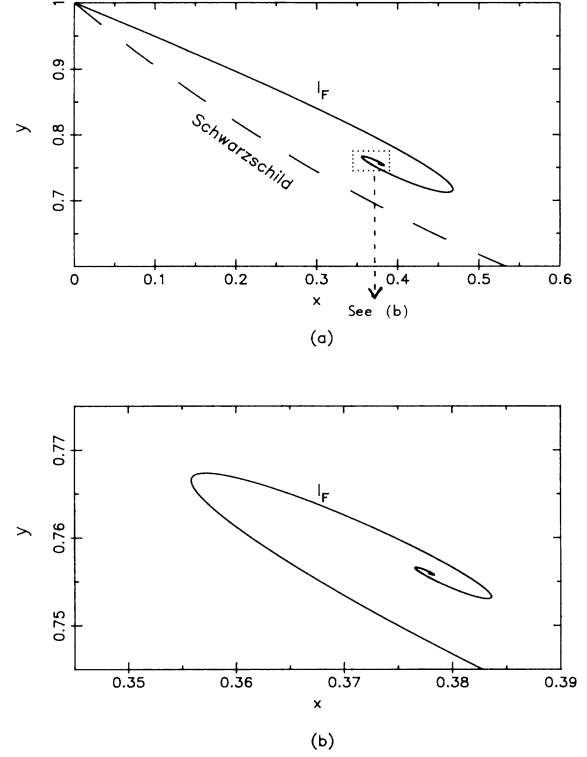


FIG. 1. The universal trajectory I_F , determined by (3.18) with the initial condition (3.22) at $x=0$ and $y=1$. The end point of I_F is $x=1/\sqrt{7}$ and $y=2/\sqrt{7}$. (The dashed curve is the Schwarzschild hyperbola $2xy + y^2 - 1 = 0$.)

At that point, the corresponding $\bar{\rho}\equiv\bar{\rho}_{\text{in}}$ is related to the stellar radius R by (3.16); therefore, after $\rho=R-$, the surface region takes over. As we shall see, just as in the case of a scalar soliton star, in the surface region when ρ increases from $R-$ to $R+$, the solution leaves I_F abruptly, moves along the straight line

$$x - x_{\text{in}} = y - y_{\text{in}}, \quad (3.27)$$

and ends at a point, called

$$A:(x_A, y_A), \quad (3.28)$$

on the Schwarzschild hyperbola

$$2xy + y^2 - 1 = 0, \quad (3.29)$$

with x_A and y_A both >0 . Afterwards, we are in the exterior region $\rho>R$, which is described by the Schwarzschild solution (2.35)–(2.37), i.e.,

$$x = \frac{2ar}{r^2 - a^2}$$

and

$$(3.30)$$

$$y = e^u = \frac{r-a}{r+a}.$$

The trajectory then moves along the hyperbola (3.29) from A when $\rho=R+$, back to point (i) when $\rho=\infty$. This is illustrated in Fig. 2. Different solutions are characterized

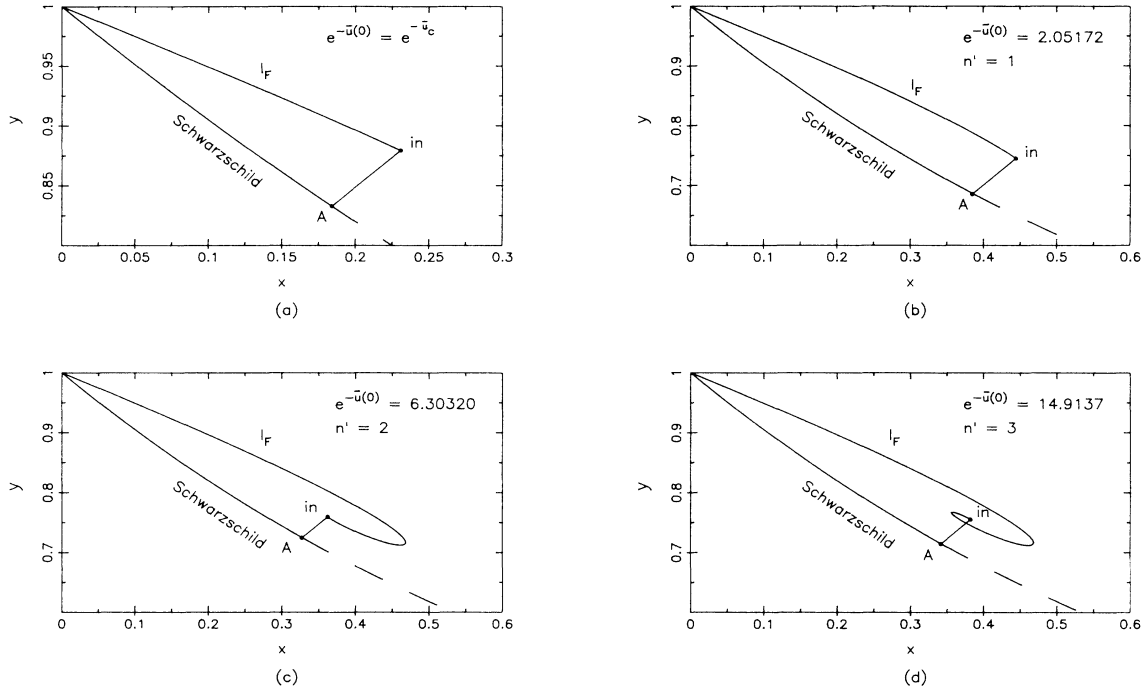


FIG. 2. Four examples of the (x, y) trajectory of the fermion soliton star solution. Each trajectory consists of three sections: (i) interior, from $x=0, y=1$ to “in” along I , (ii) surface, from “in” to A , (iii) exterior, from A back to $x=0, y=1$ along the Schwarzschild hyperbola $2xy + y^2 - 1 = 0$. (a) refers to the critical solution c of (3.59) and (3.60). (b)–(d) are the first three cusp solutions, with $n' = 1, 2$, and 3 .

only by different points (x_{in}, y_{in}) when the transition occurs; neither I_F nor the Schwarzschild hyperbola depend on the particularities of the individual solution.

As in III, we define

$$\Delta_-(x, y) = \frac{1}{3} \{ x + 2y - [(x - y)^2 + 3]^{1/2} \}. \quad (3.31)$$

It will be proved in the next section that the point “in,” defined by (3.26), is determined by $\rho = \bar{\rho}_{in} = \lambda^2 \mu R$ where $\bar{\rho}_{in}$ satisfies

$$\frac{1}{8} \bar{\rho}_{in} = \Delta_-(x(\bar{\rho}_{in}), y(\bar{\rho}_{in})). \quad (3.32)$$

C. Surface: $\rho = R + O(\mu^{-1})$

Throughout this section, we assume the fermion mass $m = |f\sigma_0|$ to be less than, or comparable to, the σ mass μ , and $\sigma_0 \sim \mu$; all three parameters are $\ll G^{-1/2}$. From (3.9) and (3.10), we see that the ratio of the surface width $\sim \mu^{-1}$ to the stellar radius R is only $(\mu R)^{-1} \sim \lambda^2$ ($\sim 10^{-34}$ if $\sigma_0 \sim \mu \sim 30$ GeV). As in the previous section, the extreme smallness of λ^2 greatly simplifies the solution within the surface. In this region it is more convenient to use the isotropic coordinates, given by (2.2). When $\rho = R$ (and therefore $\bar{\rho} = \bar{\rho}_{in}$), denote

$$\begin{aligned} u &= u_s, v = v_s, \\ r &= r_s = R e^{-v_s}. \end{aligned} \quad (3.33)$$

Within the surface $d\sigma/dr$ is $O(\mu\sigma_0)$, but because

$x = r du/dr$ and $y = 1 + r dv/dr$ are ~ 1 , du/dr and dv/dr are both $O(r_s^{-1})$, i.e., $\lambda^2 O(\mu)$. Hence, neglecting $O(\lambda^2)$, we can regard $u = u_s$ and $v = v_s$ as constants across the surface; in addition, since $S \sim mk_F^2 = \lambda O(m\mu^2)$, in the approximation $\lambda = 0+$, (2.33') becomes then

$$e^{-2v_s} \sigma'' - \frac{dU}{d\sigma} = 0. \quad (3.34)$$

This gives the solution, valid for $r = r_s + O(\mu^{-1})$,

$$\sigma = \{ 1 + \exp[\mu e^{v_s}(r - r_s)] \}^{-1} \sigma_0. \quad (3.35)$$

To the same accuracy, we have within the surface

$$U = V = O(\mu^2 \sigma_0^2)$$

but

$$W = O(\omega_F^3 m) = \lambda^{3/2} O(U). \quad (3.36)$$

By using (3.35), we find the integrals of U and V across the shell (i.e., the surface):

$$\int_{\text{shell}} U dr = \int_{\text{shell}} V dr = \frac{1}{12} \mu \sigma_0^2 e^{-v_s}. \quad (3.37)$$

Hence, in the approximation $\lambda = 0+$, we may write (valid in the surface region)

$$U = V = \frac{1}{12} \mu \sigma_0^2 e^{-v_s} \delta(r - r_s)$$

and

$$W = 0 \quad (3.38)$$

in (2.29) and (2.31); these lead to, for $r_s + > r > r_s -$,

$$\frac{dx}{dr} = \frac{dy}{dr} = -\frac{2}{3}\pi G r_s e^{v_s} \mu \sigma_0^2 \delta(r - r_s). \quad (3.39)$$

In the exterior region $r > r_s$, the same approximation $\lambda=0+$ leads to zero matter density, and therefore

$$U = V = W = 0. \quad (3.40)$$

The solution has to lie on the Schwarzschild hyperbola (3.29).

Integrating (3.39) across the surface from $r = r_s -$ to $r_s +$, we see that the discontinuities in x and y from "in" to A are

$$\Delta x = x_{\text{in}} - x_A = \frac{1}{8}\bar{\rho}_{\text{in}} = \frac{2}{3}\pi G r_s e^{v_s} \mu \sigma_0^2 \quad (3.41)$$

and

$$\Delta y = y_{\text{in}} - y_A = \frac{1}{8}\bar{\rho}_{\text{in}} = \frac{2}{3}\pi G r_s e^{v_s} \mu \sigma_0^2,$$

where $\bar{\rho}_{\text{in}} = \lambda^2 \mu R$ is given by (3.16), with $\lambda^2 = 16\pi G \sigma_0^2 / 3$ and $R = r_s e^{v_s}$. Since x_A and y_A are on the Schwarzschild hyperbola, we have

$$2x_A y_A + y_A^2 - 1 = 0. \quad (3.42)$$

Expressing x_A and y_A in terms of x_{in} , y_{in} , and $\bar{\rho}_{\text{in}}$, we derive the conditions (3.31) and (3.32).

D. Exterior: $\rho > R$

In the exterior region $\bar{\rho} > \bar{\rho}_{\text{in}}$, the Schwarzschild solution takes over: in the spherical coordinates, we have (2.35) and

$$x = \frac{2a}{\rho} \left[1 - \frac{4a}{\rho} \right]^{-1/2}, \quad y = \left[1 - \frac{4a}{\rho} \right]^{1/2}; \quad (3.43)$$

in the isotropic coordinates we have (2.36) and (3.30). In addition, ρ and r are related by

$$\rho = (r + a)^2 / r. \quad (3.44)$$

From

$$x_A = \frac{2ar_s}{r_s^2 - a^2} \quad \text{and} \quad y_A = \frac{r_s - a}{r_s + a} \quad (3.45)$$

we obtain

$$e^{u_s} = \frac{r_s - a}{r_s + a} \quad \text{and} \quad e^{v_s} = \left[\frac{r_s + a}{r_s} \right]^2. \quad (3.46)$$

Comparing e^{u_s} with the value of $e^{\bar{u}}$ at $\bar{\rho} = \bar{\rho}_{\text{in}} -$ and using (3.12), we obtain ω_F . The mass M and the radius R can be determined from $\bar{\rho}_{\text{in}} = \lambda^2 \mu R$, $r_s = R e^{-v_s}$, and x_A (or y_A). The fermion number N can be evaluated by integrating (2.16).

E. Numerical results

Following the method outlined in Sec. III A, we first assign at $\bar{\rho} = \lambda^2 m \rho = 0$ an initial value $e^{-\bar{u}(0)}$, in accordance with (3.15). The two coupled first-order differential equations (3.13) are then integrated from $\bar{\rho} = 0$ to $\bar{\rho} > 0$. The

actual task of integration can be facilitated by observing the invariance of (3.13) under the transformation

$$e^{-\bar{u}} \rightarrow \kappa e^{-\bar{u}}, \quad \bar{\rho} \rightarrow \bar{\rho} / \kappa^2, \quad \bar{v} \rightarrow \bar{v}, \quad (3.47)$$

where κ is a constant. Of course, the boundary condition (3.15) must vary accordingly, with

$$\bar{u}(0) \rightarrow \bar{u}(0) - \ln \kappa. \quad (3.48)$$

Consequently, solutions with different initial values $e^{-\bar{u}(0)}$ are related to each other.

Define $\hat{u}(\hat{\rho})$ and $\hat{v}(\hat{\rho})$ to be the solution of

$$2\hat{\rho} d\hat{v} / d\hat{\rho} = (e^{-4\hat{u}} \hat{\rho}^2 - 1) e^{2\hat{v}} + 1 \quad (3.49)$$

and

$$2\hat{\rho} d\hat{u} / d\hat{\rho} = (\frac{1}{3} e^{-4\hat{u}} \hat{\rho}^2 + 1) e^{2\hat{v}} - 1,$$

with the boundary condition

$$\hat{u} = \hat{v} = 0 \quad \text{at} \quad \hat{\rho} = 0. \quad (3.50)$$

Any solution of (3.13) with the boundary condition $\bar{u}(0) \neq 0$ can then be derived from $\hat{u}(\hat{\rho})$ and $\hat{v}(\hat{\rho})$ through

$$\exp[-\bar{u}(\bar{\rho})] = \exp[-\hat{u}(\hat{\rho}) - \bar{u}(0)] \quad (3.51)$$

and

$$\exp[-\bar{v}(\bar{\rho})] = \exp[-\hat{v}(\hat{\rho})],$$

where

$$\bar{\rho} = \hat{\rho} e^{2\bar{u}(0)}. \quad (3.52)$$

Because $y = e^{-\bar{v}}$ and $x = y\bar{\rho} d\bar{u} / d\bar{\rho}$, we have

$$y = e^{-\hat{v}}, \quad x = y\hat{\rho} d\hat{u} / d\hat{\rho}. \quad (3.53)$$

Thus, from $\hat{u}(\hat{\rho})$ and $\hat{v}(\hat{\rho})$, we also derive $x(\hat{\rho})$ and $y(\hat{\rho})$. These four functions are plotted in Fig. 3.

In order to have a solution of the fermion soliton star, we must satisfy (3.32):

$$\frac{1}{8}\hat{\rho} = \Delta_-(x, y), \quad (3.54)$$

where $\Delta_-(x, y)$ is given by (3.31). Substituting the solutions $x(\hat{\rho})$ and $y(\hat{\rho})$ into (3.31) we define

$$\Delta_-(\hat{\rho}) \equiv \Delta_-(x(\hat{\rho}), y(\hat{\rho})); \quad (3.55)$$

hence, (3.54) becomes

$$\frac{1}{8} e^{2\bar{u}(0)} \hat{\rho} = \Delta_-(\hat{\rho}), \quad (3.56)$$

whose solution $\hat{\rho} = \hat{\rho}_{\text{in}}$ determines a $\bar{\rho}_{\text{in}}$ through (3.52); i.e.,

$$\bar{\rho}_{\text{in}} = \hat{\rho}_{\text{in}} e^{2\bar{u}(0)}. \quad (3.57)$$

From (3.26) and (3.41), it follows that

$$\begin{aligned} x_{\text{in}} &= x(\hat{\rho}_{\text{in}}), \quad y_{\text{in}} = y(\hat{\rho}_{\text{in}}), \\ x_A &= x_{\text{in}} - \Delta_-(\hat{\rho}_{\text{in}}), \quad y_A = y_{\text{in}} - \Delta_-(\hat{\rho}_{\text{in}}). \end{aligned} \quad (3.58)$$

These and (3.45) and (3.46) then determine M , R , r_s , and other physical characteristics of the soliton star.

In Fig. 4 the solid curve is $\Delta_-(\hat{\rho})$ which is independent of $e^{-\bar{u}(0)}$, and the dashed line is $e^{2\bar{u}(0)} \hat{\rho} / 8$. For $e^{-\bar{u}(0)} = 2.5$, there are two solutions of (3.56). It is clear

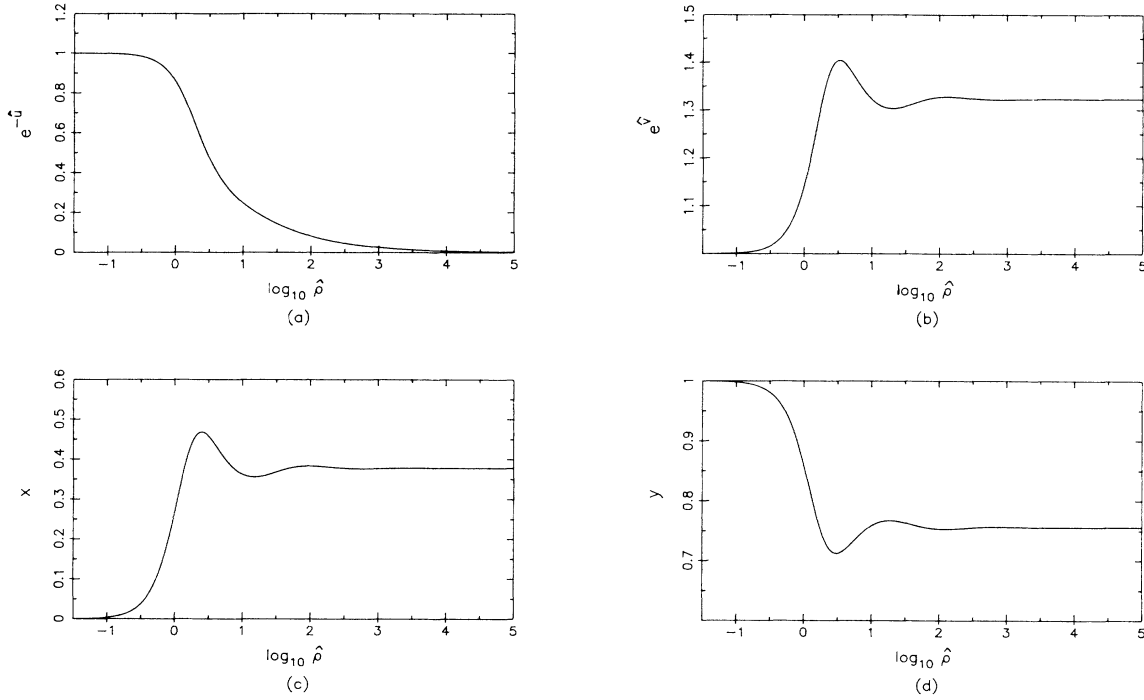


FIG. 3. From the solutions of $\hat{u}(\hat{\rho})$, $\hat{v}(\hat{\rho})$, $x(\hat{\rho})$, and $y(\hat{\rho})$ of (3.49), (3.50), and (3.53), one can derive $\bar{u}(\bar{\rho})$, $\bar{v}(\bar{\rho})$, $x(\bar{\rho})$, and $y(\bar{\rho})$ through (3.51) and (3.52), for any initial value $\bar{u}(0)$.

that if we decrease $e^{-\bar{u}(0)}$, the dashed line will swing counterclockwise, until it reaches a critical point, called c , when

$$e^{-u(0)} = e^{-\bar{u}_c} = 1.6204941. \tag{3.59}$$

At c , (3.56) has only one unique solution; its physical characteristics are

$$\begin{aligned} \omega_F &= 2.2628\pi^{3/4}G^{1/4}\mu^{1/2}\sigma_0, \\ N &= 3.9869 \times 10^{-3} / \pi^{7/4}G^{9/4}\mu^{3/2}\sigma_0^3, \\ M &= 1.0796 \times 10^{-2} / \pi G^2\mu\sigma_0^2, \\ R &= 7.0221 \times 10^{-2} / \pi G\mu\sigma_0^2, \\ \bar{\rho}_{in} &= 0.37451, \quad e^{-u(0)} = 1.3908. \end{aligned} \tag{3.60}$$

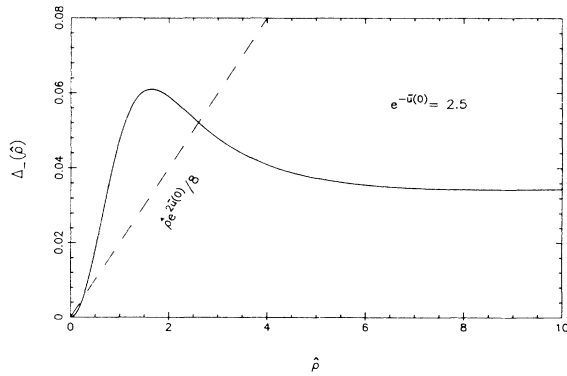


FIG. 4. The solid curve is $\Delta_-(\hat{\rho})$ defined by (3.55). The initial value $e^{-\bar{u}(0)}$ determines the slope of the dashed line, $\frac{1}{8}e^{2\bar{u}(0)}\hat{\rho}$, whose intersection with $\Delta_-(\hat{\rho})$ gives a solution of the fermion soliton star, in accordance with (3.56) and (3.57).

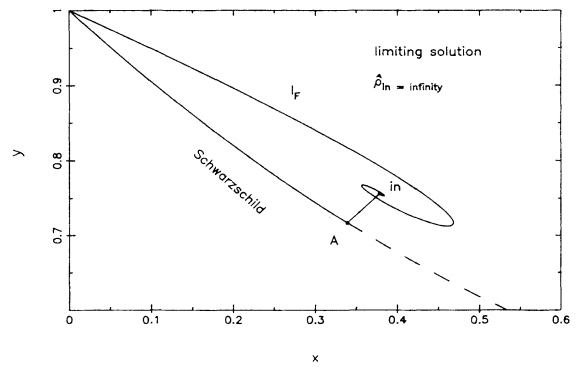


FIG. 5. (x, y) trajectory of the limiting case L for the soliton star when $e^{-\bar{u}(0)} \rightarrow \infty$ and $\hat{\rho}_{in} \rightarrow \infty$. The point “in” is at $x = 1/\sqrt{7}$ and $y = 2/\sqrt{7}$; therefore the upper curve consists of the entire universal trajectory I_F .

TABLE I. Physical characteristics of the first six cusps for the fermion soliton star solutions.

n'	$e^{-\bar{u}(0)}$	$\bar{\rho}_{\text{in}}$	$\omega_F/\pi^{3/4}G^{1/4}\mu^{1/2}\sigma_0$	$\pi^{7/4}G^{9/4}\mu^{3/2}\sigma_0^2N$	$\pi G^2\mu\sigma_0^2M$	R/GM
1	2.051 72	0.472 797	1.747 66	$1.028\ 33\times 10^{-2}$	$2.335\ 40\times 10^{-2}$	3.795 90
2	6.303 20	0.276 939	2.098 89	$4.331\ 66\times 10^{-3}$	$1.233\ 52\times 10^{-2}$	4.209 59
3	14.913 7	0.321 248	1.996 88	$5.491\ 50\times 10^{-3}$	$1.471\ 94\times 10^{-2}$	4.092 16
4	37.807 5	0.309 723	2.021 67	$5.178\ 96\times 10^{-3}$	$1.409\ 22\times 10^{-2}$	4.120 93
5	94.209 3	0.312 617	2.015 34	$5.256\ 73\times 10^{-3}$	$1.424\ 93\times 10^{-2}$	4.113 59
6	235.780	0.311 884	2.016 93	$5.236\ 98\times 10^{-3}$	$1.420\ 95\times 10^{-2}$	4.115 44

The corresponding (x,y) trajectory is given in Fig. 2(a).

For $e^{-\bar{u}(0)} < e^{-\bar{u}_c}$, there is no solution; for $e^{-\bar{u}(0)} > e^{-\bar{u}_c}$, there are two solutions. When

$$e^{-\bar{u}(0)} \rightarrow \infty, \quad (3.61)$$

one of the solutions has $\hat{\rho}_{\text{in}} \rightarrow \infty$, as can be inferred from Fig. 4; this solution will be referred to as L , the limiting solution. (The product $\bar{\rho}_{\text{in}} = \hat{\rho}_{\text{in}} e^{2\bar{u}(0)}$ remains finite.) The (x,y) trajectory of L is shown in Fig. 5; in this case, the point “in” is at $x = 1/\sqrt{7}$ and $y = 2/\sqrt{7}$. The various physical characteristics of L are

$$\begin{aligned} x_A &= \frac{1}{3\sqrt{7}}(-2 + \sqrt{22}), \quad y_A = \frac{1}{3\sqrt{7}}(1 + \sqrt{22}), \\ \bar{\rho}_{\text{in}} &= \frac{8}{3\sqrt{7}}(5 - \sqrt{22}), \\ \omega_F &= \left(\frac{2}{27}\right)^{1/4} [7(5 - \sqrt{22})]^{-1/2} (1 + \sqrt{22}) \pi^{3/4} G^{1/4} \mu^{1/2} \sigma_0, \\ N &= \left(\frac{1}{21}\right) \left(\frac{1}{6}\right)^{1/4} (5 - \sqrt{22})^{3/2} / \pi^{7/4} G^{9/4} \mu^{3/2} \sigma_0^3, \quad (3.62) \\ M &= \frac{122 - 25\sqrt{22}}{126\sqrt{7}} / \pi G^2 \mu \sigma_0^2, \\ \frac{R}{GM} &= \frac{63}{20 - \sqrt{22}} = 4.115\ 069. \\ \frac{r_s}{GM} &= \frac{1}{2} \left[\frac{3\sqrt{7} + 1 + \sqrt{22}}{3\sqrt{7} - 1 - \sqrt{22}} \right] = 3.032\ 63. \end{aligned}$$

By systematically changing $e^{-\bar{u}(0)}$, we can survey all the solutions. In Figs. 6(a) and 6(b), M is plotted versus N , schematically in 6(a) and precisely in 6(b). As in II and III, it shows the typical pattern of cusps, which are labeled consecutively, $n'=1,2,3,\dots$. The (x,y) trajectories of the first three cusps $n'=1,2$, and 3 are given in Figs. 2(b)–2(d). The physical characteristics of the first six cusps are listed in Table I.

As representatives of the extensive analysis that has been made, we show in Fig. 7 the curves M vs ω_F , N vs ω_F , R vs ω_F , and R vs M , and in Fig. 8 the dependences of $e^{\bar{u}(0)}$, M , ω_F , and R on $\hat{\rho}_{\text{in}}$.

IV. BLACK HOLES

A. General discussion

Throughout this section, we adopt the approximation regarding $\lambda = 4\sigma_0(\pi G/3)^{1/2}$ as an infinitesimal. (λ is $\sim 10^{-17}$ for $\sigma_0 \sim 30$ GeV.) The region $r < r_s$, where the

matter density is nonzero, will be referred to as the inside of the star, and $r > r_s$ as its outside. For the black-hole solution, the stellar radius r_s is $< a = \frac{1}{2}GM$, the Schwarzschild radius in the isotropic coordinates. We call $r < a$ inside the black hole, and $r > a$ its outside.

To obtain the solution inside the star we follow the same steps as in Sec. III A. First assign an initial value $e^{-\bar{u}(0)}$, then integrate (3.13) from $\bar{\rho}=0$ outwards. Using $x = y\bar{\rho}d\bar{u}/d\bar{\rho}$ and $y = e^{-\bar{v}}$, we determine $x = x(\bar{\rho})$ and $y = y(\bar{\rho})$, as before. Define [instead of (3.31)]

$$\Delta_+(x,y) \equiv \frac{1}{3} \{ x + 2y + [(x-y)^2 + 3]^{1/2} \}. \quad (4.1)$$

The interior solution of a star stops at $\bar{\rho} = \bar{\rho}_{\text{in}}$, determined now by [instead of (3.32)]

$$\frac{1}{8}\bar{\rho}_{\text{in}} = \Delta_+(x(\bar{\rho}_{\text{in}}), y(\bar{\rho}_{\text{in}})). \quad (4.2)$$

Let

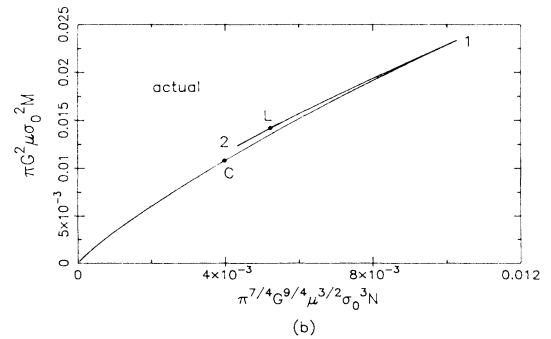
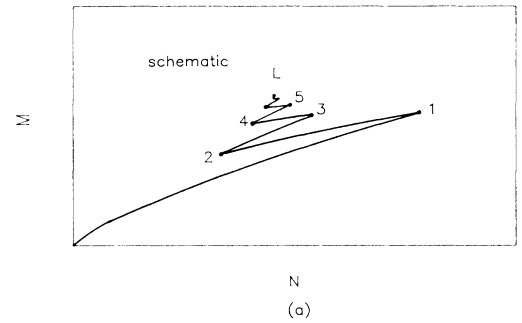


FIG. 6. Fermion soliton star mass M vs the particle number N : a schematic drawing in (a) and the actual plot in (b). (The labels 1,2,... refer to the consecutive cusp number $n'=1,2,\dots$, with L standing for $n'=\infty$.)

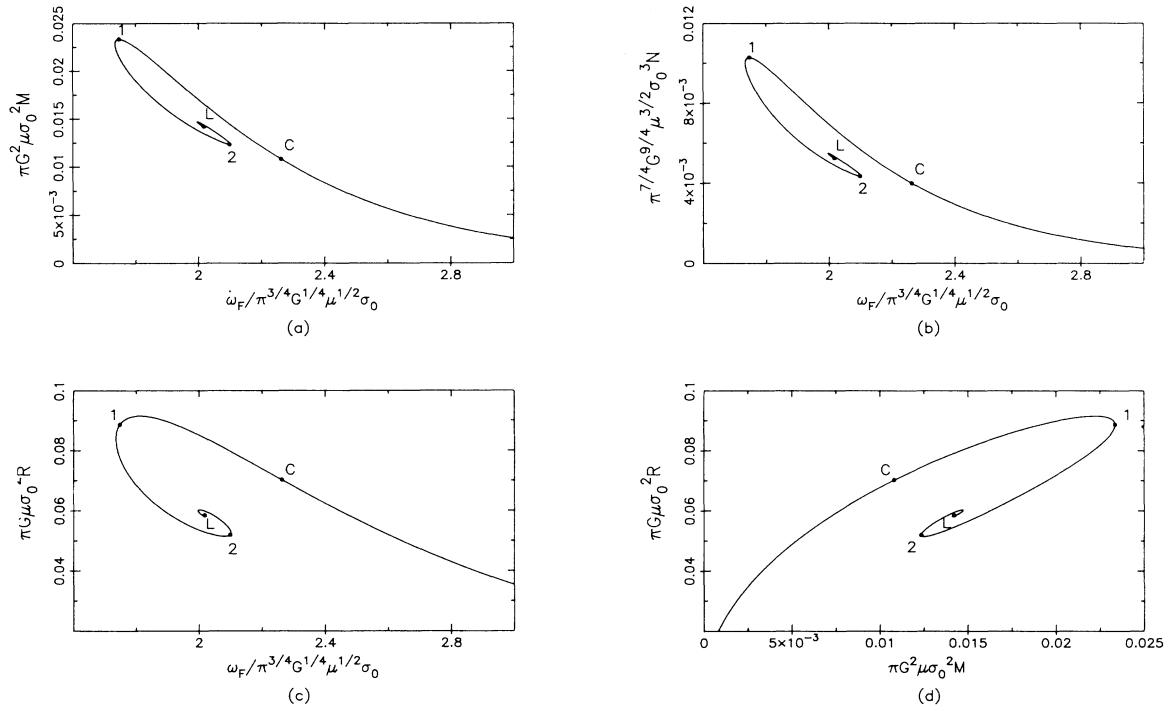


FIG. 7. M vs ω_F in (a), N vs ω_F in (b), R vs ω_F in (c), and R vs M in (d).

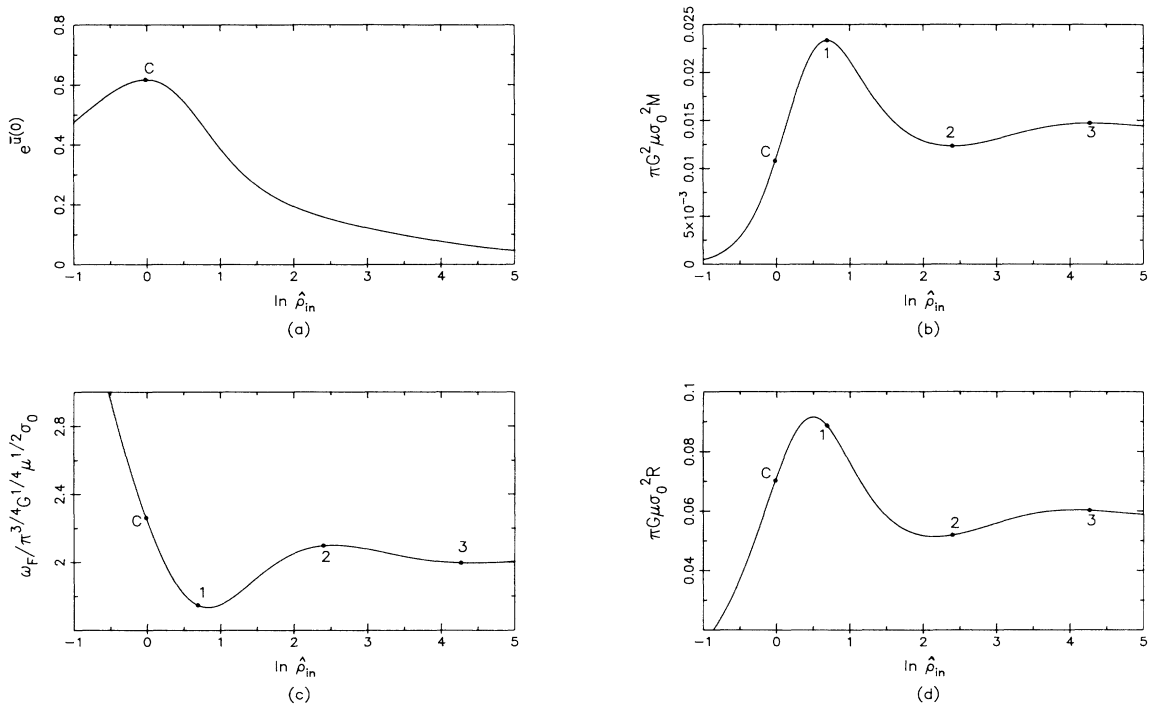


FIG. 8. $e^{u(0)}$ vs $\hat{\rho}_{in}$ in (a), M vs $\hat{\rho}_{in}$ in (b), ω_F vs $\hat{\rho}_{in}$ in (c), and R vs $\hat{\rho}_{in}$ in (d), where $\hat{\rho}_{in}$ is defined by (3.57).

$$x_{\text{in}} \equiv x(\bar{\rho}_{\text{in}}) \quad \text{and} \quad y_{\text{in}} \equiv y(\bar{\rho}_{\text{in}}). \quad (4.3)$$

Equation (4.2) ensures that the point B , with

$$x_B \equiv x_{\text{in}} - \frac{1}{8}\bar{\rho}_{\text{in}} \quad (4.4)$$

and

$$y_B \equiv y_{\text{in}} - \frac{1}{8}\bar{\rho}_{\text{in}},$$

lies on the Schwarzschild hyperbola (3.29) with

$$x_B < 0, \quad y_B < 0. \quad (4.5)$$

Except for the sign change between $\Delta_-(x,y)$ of (3.31) and $\Delta_+(x,y)$ of (4.1), the procedure for deriving a black-hole solution is essentially the same as that for the soliton star. As in (3.16), the star radius in the spherical coordinates is given by

$$\rho = R = \bar{\rho}_{\text{in}}/\mu\lambda^2. \quad (4.6)$$

From the Schwarzschild solution, we have

$$\begin{aligned} x_B &= \frac{2ar_s}{r_s^2 - a^2}, \\ y_B &= \frac{r_s - a}{r_s + a}, \\ R &= \frac{(r_s + a)^2}{r_s}; \end{aligned} \quad (4.7)$$

consequently, r_s , a , and M can also be determined. Because x_B and y_B are negative, we have $r_s < a$; i.e., the radius of the star is smaller than the Schwarzschild radius (in the isotropic coordinates).

The (x,y) trajectory of the black hole is then completely determined. From $r=0$ to $r=r_s-$, it follows I_F up to $(x_{\text{in}}, y_{\text{in}})$; this is the inside of the star. From $r=r_s-$ to r_s+ it travels from $(x_{\text{in}}, y_{\text{in}})$ to (x_B, y_B) along a straight line, and thereby sweeps over the surface region. Outside the star, the Schwarzschild solution takes over; the (x,y) trajectory follows the hyperbola $2xy + y^2 - 1 = 0$ from B at $r=r_s+$ to $x=-\infty, y=0$ which is the inner face of the horizon $r=a = \frac{1}{2}GM$, then switches to $x=\infty, y=0$ the outer face of the horizon, and back to $x=0, y=1$ (when $r=\infty$) along the $x>0, y>0$ branch of the Schwarzschild hyperbola. This is illustrated in Fig. 9.

B. The sign of e^u

In the exterior of the star $r > r_s$, there is no matter density; therefore, the Schwarzschild solution holds:

$$\begin{aligned} e^u &= \frac{r-a}{r+a}, \quad e^v = \left(\frac{r+a}{r} \right)^2, \\ e^{\bar{v}} &= e^{-u}. \end{aligned} \quad (4.8)$$

Hence, while e^u is positive for $r > a$, it becomes negative for $r < a$, i.e., inside the black hole. Einstein's equation for free space, $u'' + v'' + v'^2 + r^{-1}(u' + v') = 0$, requires u' to be continuous; therefore e^u changes sign at $r = a \pm$. Since e^u is continuous at the surface of the star $r = r_s$, e^u is also < 0 inside the star. In contrast, e^v is positive

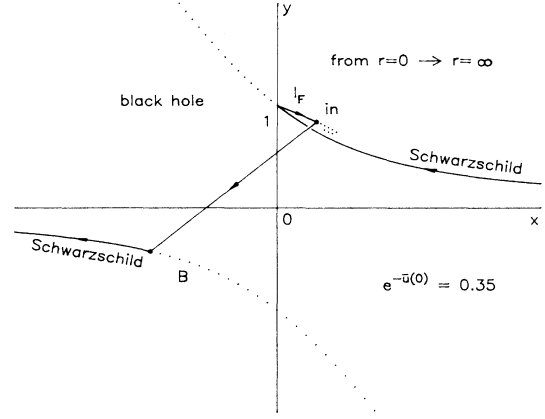


FIG. 9. Example of a (x,y) trajectory of a black-hole solution, with the arrow in the direction of increasing r (the radius in the isotropic coordinates).

everywhere.

As already discussed in III, the sign of e^u can also be inferred from the mass formula

$$M = M_{\text{space}} + M_{\text{star}}, \quad (4.9)$$

where

$$\begin{aligned} M_{\text{space}} &\equiv \int_{r_s+}^{\infty} \mathcal{E} dr, \\ M_{\text{star}} &\equiv \int_0^{r_s+} \mathcal{E} dr, \\ \mathcal{E} &= e^u r^2 [4\pi e^{3v}(U + V + W) - (2G)^{-1} e^v v'(2u' + v')]. \end{aligned} \quad (4.10)$$

Because $M_{\text{space}} = Ma/r_s > M$, we must have $M_{\text{star}} < 0$, in agreement with $e^u < 0$ inside the star. The sign of e^u implies that under an infinitesimal time translation dt , the line element $e^u dt$ has opposite signs on the two sides of the horizon. Hence, one may regard the direction of time flow as also changing sign across the horizon (with respect to an appropriate overall frame).

Because k_F the Fermi momentum and ϵ_F the Fermi energy are, by definition, positive, we have

$$\omega_F < 0 \quad (4.12)$$

on account of (2.32). From (3.15), we see that the sign of $e^{-\bar{u}(0)}$ is positive.

C. Numerical results

Define $\hat{\rho}$ by (3.52), and let $\hat{u}(\hat{\rho})$ and $\hat{v}(\hat{\rho})$ be the same solution of (3.49) with the boundary condition (3.50). By using $y(\hat{\rho}) = \exp[-\hat{v}(\hat{\rho})]$ and $x(\hat{\rho}) = y\hat{\rho} d\hat{u}/d\hat{\rho}$, we define, in terms of $\Delta_+(x,y)$ given by (4.1),

$$\Delta_+(\hat{\rho}) \equiv \Delta_+(x(\hat{\rho}), y(\hat{\rho})) \quad (4.13)$$

which is obviously independent of $e^{\bar{u}(0)}$. For each solution $\hat{\rho} = \hat{\rho}_{\text{in}}$ of

$$\frac{1}{8} e^{2\bar{u}(0)} \hat{\rho} = \Delta_+(\hat{\rho}), \quad (4.14)$$

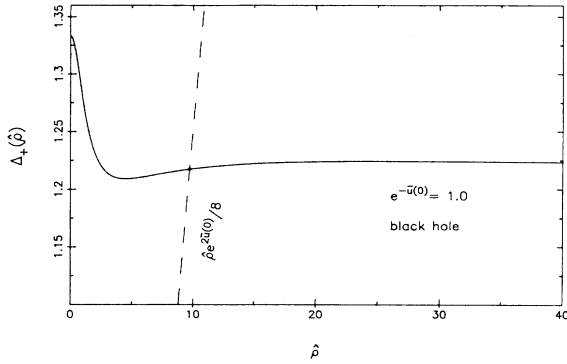


FIG. 10. Solid curve is $\Delta_+(\hat{\rho})$ defined by (4.13); its intersection with the dashed line $e^{2\bar{u}(0)}\hat{\rho}/8$ gives the solution $\hat{\rho}=\hat{\rho}_{in}$, in accordance with (4.14).

a solution of the black hole can be derived, with

$$\begin{aligned} x_{in} &= x(\hat{\rho}_{in}), \quad y_{in} = y(\hat{\rho}_{in}), \\ x_B &= x_{in} - \frac{1}{8}\bar{\rho}_{in} = \frac{2ar_s}{r_s^2 - a^2} < 0, \\ y_B &= y_{in} - \frac{1}{8}\bar{\rho}_{in} = \frac{r_s - a}{r_s + a} < 0, \\ \bar{\rho}_{in} &= \hat{\rho}_{in}e^{2\bar{u}(0)}, \quad R = r_s e^{v_s}, \\ e^{u_s} &= \frac{r_s - a}{r_s + a}, \quad e^{v_s} = \left[\frac{r_s + a}{r_s} \right]^2, \end{aligned} \tag{4.15}$$

and, as before, the Schwarzschild radius in the isotropic coordinates is

$$a = \frac{1}{2}GM.$$

The function $\Delta_+(\hat{\rho})$ is shown in Fig. 10. From its shape, one sees that for any given $e^{\bar{u}(0)}$, there is one and only one solution of (4.14). When $e^{-\bar{u}(0)} \rightarrow \infty$, we have

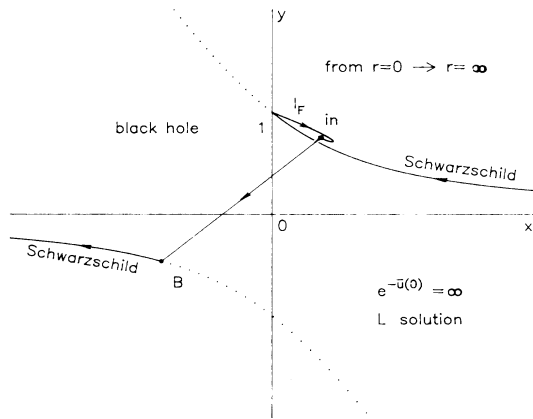


FIG. 11. The (x,y) trajectory of the (limiting) L solution for a fermion black hole. See (4.16) for a description of the L solution.

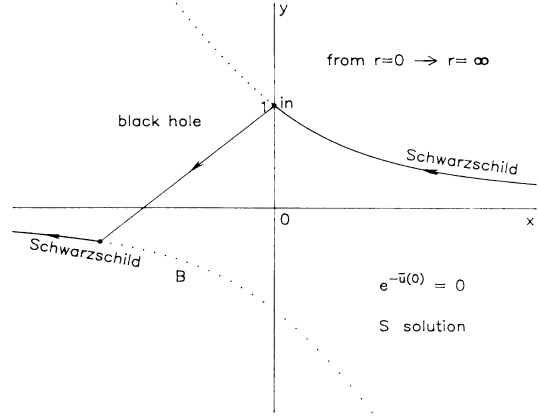


FIG. 12. The (x,y) trajectory of the (shell) S solution for a fermion black hole. For $r < r_s$, the space is flat; at $r = r_s = \frac{1}{2}a$, there is a shell of matter, and for $r > r_s$ one has the Schwarzschild solution, with the horizon located at $r = a = \frac{1}{2}GM$, where $M = 8/9\pi G^2\mu\sigma_0^2$.

the limiting solution L , whose physical characteristics are

$$\begin{aligned} x_{in} &= 1/\sqrt{7}, \quad y_{in} = 2/\sqrt{7}, \\ x_B &= -\frac{1}{3\sqrt{7}}(2 + \sqrt{22}), \quad y_B = -\frac{1}{3\sqrt{7}}(-1 + \sqrt{22}), \\ r_s &= \frac{122 + 25\sqrt{22}}{252\sqrt{7}} \left[\frac{3\sqrt{7} + 1 - \sqrt{22}}{3\sqrt{7} - 1 + \sqrt{22}} \right] GM = 0.131067GM, \\ R &= \frac{63}{20 + \sqrt{22}} GM = 2.55160GM, \\ \omega_F &= -\left(\frac{2}{27}\right)^{1/4} [7(5 + \sqrt{22})]^{-1/2} (\sqrt{22} - 1) \pi^{3/4} G^{1/4} \mu^{1/2} \sigma_0, \\ N &= \frac{1}{21} \left(\frac{1}{6}\right)^{1/4} (5 + \sqrt{22})^{3/2} / \pi^{7/4} G^{9/4} \mu^{3/2} \sigma_0^3, \\ M &= \frac{122 + 25\sqrt{22}}{126\sqrt{7}} / \pi G^2 \mu \sigma_0^2. \end{aligned} \tag{4.16}$$

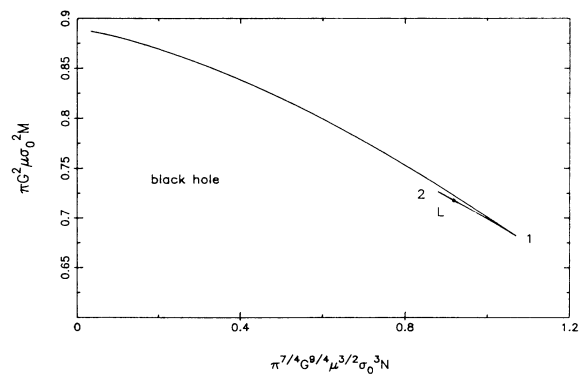


FIG. 13. M vs N for the fermion black-hole solution, with $n'=1, 2, \dots$ denoting the successive cusps, and $n'=\infty$ the L solution.

TABLE II. Physical characteristics of the first five cusp solutions ($n'=1, 2, \dots, 5$) of black holes. Here, $n'=0$ and $n'=\infty$ refer to the S solution and the L solution.

n'	$e^{-\bar{u}(0)}$	$\omega_F/\pi^{3/4}G^{1/4}\mu^{1/2}\sigma_0$	$\pi^{7/4}G^{9/4}\mu^{3/2}\sigma_0^3N$	$\pi G\mu\sigma_0^2r_s$	$\pi G^2\mu\sigma_0^2M$
0	0	0	0	$\frac{2}{9}$	$\frac{8}{9}$
1	0.5734	-0.26291	1.07001	0.11355	0.68190
2	1.4158	-0.22664	0.87964	0.13557	0.72662
3	3.5589	-0.23557	0.92747	0.12993	0.71546
4	8.8885	-0.23330	0.91538	0.13135	0.71828
5	22.233	-0.23388	0.91844	0.13099	0.71757
∞	∞	-0.23376	0.91782	0.13107	0.71771

The (x,y) trajectory of the L solution is shown in Fig. 11.

As in III, when the initial value $e^{-\bar{u}(0)} \rightarrow 0$, there is another limiting solution, which may be called the S solution (or, shell solution): the point “in” of the S solution is at $x=0$ and $y=1$; correspondingly, we have $x_B = -\frac{4}{3}$, $y_B = -\frac{1}{3}$, $M = 8/9\pi G^2\mu\sigma_0^2$, and $r_s = 2/9\pi G\mu\sigma_0^2$ but $N = \omega_F = 0$. Consequently, the matter energy is due entirely to the $U + V$ term on the surface of the star. Inside the black hole there is a shell of scalar field matter located at $r = r_s = 2/9\pi G\mu\sigma_0^2 = \frac{1}{2}a$ (with the horizon at $r = a = \frac{1}{2}GM$), and inside the shell, for $r < r_s$, we have a flat space with $e^{-u} = -3$, $e^{-v} = \frac{1}{9}$, $e^{-\bar{v}} = 1$, and $e^{-\bar{u}} \propto \omega_F e^{-u}/\lambda m = 0$. The (x,y) trajectory of the S solution is shown in Fig. 12.

In Fig. 13 we give the mass M of the black hole versus its particle number N . Again, it has an infinite number of cusps, which will be labeled consecutively by $n'=1, 2, 3, \dots$. The slope $dM/dN = \omega_F$ is negative, in

agreement with (4.12); in contrast, for the soliton star solution of Sec. III, the corresponding slope dM/dN is positive. The physical characteristics of the first five cusp solutions are given in Table II. The limiting solution L refers to $n' \rightarrow \infty$ (and also $e^{-\bar{u}(0)} \rightarrow \infty$).

In Fig. 14 we plot ω_F vs N , ω_F vs r_s , M vs r_s , and M vs r_s/a . We see that the ratio of the star radius r_s to the Schwarzschild radius $a = \frac{1}{2}GM$ (in the isotropic coordinates) is always < 1 , as expected. Figure 15 illustrates the relation between the circumference $2\pi\rho$ of a two-sphere and the radius r in the isotropic coordinates for the black-hole solution.

An interesting mathematical limit is to set

$$m \rightarrow \infty \quad \text{and} \quad \mu \rightarrow \infty, \quad (4.17)$$

but maintain intact the relation (1.3)

$$m - f\sigma_0 = 0$$

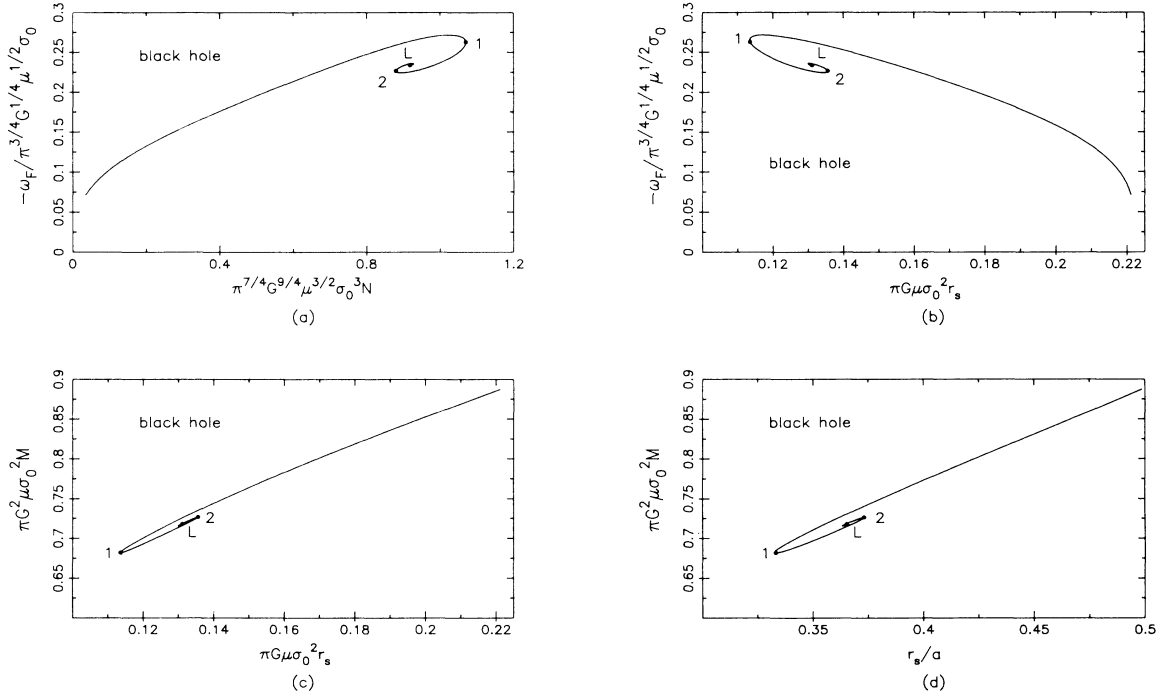


FIG. 14. ω_F vs N in (a), ω_F vs r_s in (b), M vs r_s in (c), and M vs r_s/a in (d) for the fermion black-hole solution.

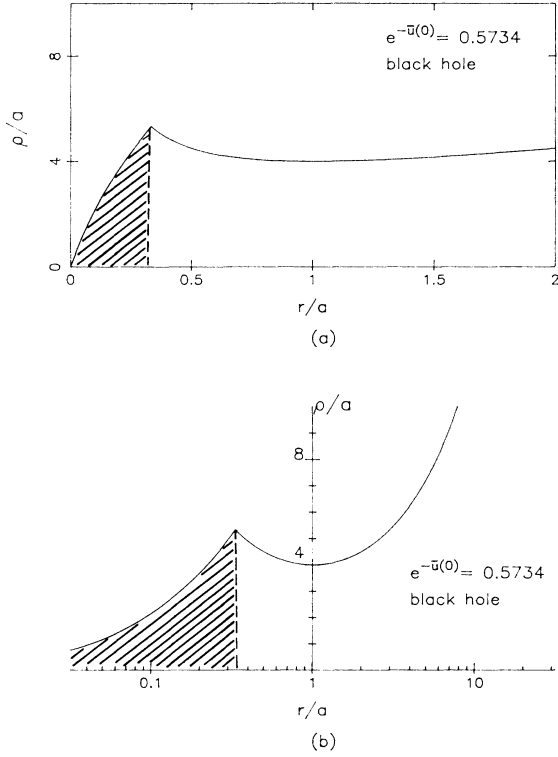


FIG. 15. ρ vs r for the $n'=1$ fermion black-hole solution, with (a) in a linear scale of r and (b) in a logarithmic scale. The matter distribution is located in the shaded region with $r \leq r_s$, and the horizon is at $r/a=1$. Outside the star $r > r_s$, we have the Schwarzschild solution $\rho/a = [(r/a)^{1/2} + (a/r)^{1/2}]^2$.

and keep fixed Newton's constant G and the surface tension

$$s \equiv \frac{1}{6} \mu \sigma_0^2 = \text{finite} \neq 0; \quad (4.18)$$

hence, $\sigma_0=0$ and, from (3.10), $\lambda=0$. From Table II, it follows that all overall physical parameters of the solution, such as ω_F , N , r_s , M , and $a = \frac{1}{2} GM$ stay the same, since they depend only on G and s . In this limit, outside the star, $r > r_s$, the Schwarzschild solution becomes exact, because in that region σ , W , U , and V are all zero (without approximation). This, then, provides a convenient alternative way to bypass the complication discussed in the second remark of Sec. IV F in paper III.

V. REMARKS

Recent progress in particle physics points out the importance of nonlinearity and coherence in the realm of 10^{-13} – 10^{-17} cm, as exemplified by the QCD vacuum in connection with quark confinement and the role of Higgs fields in electroweak symmetry breaking. Assuming that these overall phenomena may be effectively represented by scalar fields, it seems reasonable that such coherence can be accumulated and extended to macroscopic and even to astronomical distances. The explicit model solutions derived here are meant to demonstrate the feasibility, at least in principle.

The extension to gauge fields will be given in a subsequent paper.

At present, there is no experimental evidence that soliton stars exist. Nevertheless, it seems reasonable that solutions of well-tested theories, such as Einstein's general relativity, the Dirac equation, the Klein-Gordon equation, etc., should find their proper place in nature.

ACKNOWLEDGMENTS

One of us (T.D.L.) wishes to thank the members of the CERN Theory Division for their kind hospitality when most of this paper was written. This research was supported in part by the U.S. Department of Energy.

APPENDIX

In this appendix we give the derivation of the Thomas-Fermi approximation used in Secs. II A and II B.

1. Lagrangian

At each point in space, we set up a vierbein of four (real) basis vectors e_α^μ and their inverse ϵ_μ^α ; they satisfy

$$\begin{aligned} g_{\mu\nu} &= \epsilon_\mu^\alpha \epsilon_\nu^\beta \eta_{\alpha\beta}, \\ g^{\mu\nu} &= e_\alpha^\mu e_\beta^\nu \eta^{\alpha\beta}, \end{aligned} \quad (A1)$$

$$e_\alpha^\mu \epsilon_\nu^\alpha = \delta_\nu^\mu = \begin{cases} 0 & \text{if } \mu \neq \nu, \\ 1 & \text{if } \mu = \nu, \end{cases}$$

$$\text{matrix } \eta_{\mu\nu} = \begin{pmatrix} -1 & 0 & 0 & 0 \\ 0 & 1 & 0 & 0 \\ 0 & 0 & 1 & 0 \\ 0 & 0 & 0 & 1 \end{pmatrix}.$$

The covariant derivative of a fermion field ψ is

$$D_\mu \psi = \left[\frac{\partial}{\partial x^\mu} + \Gamma_\mu \right] \psi, \quad (A2)$$

where Γ_μ and the Dirac matrices γ_μ satisfy

$$\begin{aligned} \{\gamma^\mu, \gamma^\nu\} &= 2g^{\mu\nu}, \\ \{\gamma_\mu, \gamma_\nu\} &= 2g_{\mu\nu}, \\ \{\gamma^\mu, \gamma_\nu\} &= 2\delta_\nu^\mu, \\ \gamma^\mu &= g^{\mu\nu} \gamma_\nu, \end{aligned} \quad (A3)$$

$$[\gamma_\mu, \Gamma_\nu] = \frac{\partial \gamma_\mu}{\partial x^\nu} - \Gamma_{\mu\nu}^\alpha \gamma_\alpha,$$

and $\Gamma_{\mu\nu}^\alpha$ is the Christoffel symbol:

$$\Gamma_{\mu\nu}^\alpha = \frac{1}{2} g^{\alpha\beta} \left[\frac{\partial g_{\beta\nu}}{\partial x^\mu} + \frac{\partial g_{\beta\mu}}{\partial x^\nu} - \frac{\partial g_{\mu\nu}}{\partial x^\beta} \right].$$

In addition, we require the Hermitian of γ_μ to be

$$\gamma_\mu^\dagger = \sum_{\alpha=0}^3 \epsilon_\mu^\alpha \epsilon_\nu^\alpha \gamma^\nu. \quad (A4)$$

The part of the Lagrangian density that contains the fermion field is

$$\mathcal{L}(f) = \frac{1}{2} \left[\frac{\partial \bar{\psi}}{\partial x^\mu} \gamma^\mu \psi - \bar{\psi} \gamma^\mu \frac{\partial \psi}{\partial x^\mu} \right] - \frac{1}{2} \bar{\psi} (\gamma^\mu \Gamma_\mu + \Gamma_\mu \gamma^\mu) \psi - (m - f\sigma) \bar{\psi} \psi, \quad (\text{A5})$$

where $\bar{\psi}$ is the adjoint of ψ . [See (A16) below.] Hence, the Dirac equation is

$$\gamma^\mu D_\mu \psi + (m - f\sigma) \psi = 0. \quad (\text{A6})$$

The current j^μ is given by

$$j^\mu \equiv i \bar{\psi} \gamma^\mu \psi. \quad (\text{A7})$$

From the Dirac equation, one sees that j^μ satisfies the conservation law

$$j^\mu_{;\mu} = \frac{\partial}{\partial x^\mu} (|g|^{1/2} j^\mu) = 0, \quad (\text{A8})$$

where, as before,

$$|g| = \text{absolute value of the determinant of the matrix } g_{\mu\nu}. \quad (\text{A9})$$

In what follows we shall restrict our discussions to the time-independent spherically symmetric metric $g_{\mu\nu}$, defined by

$$ds^2 = -e^{2u} dt^2 + e^{2v} (dx^2 + dy^2 + dz^2); \quad (\text{A10})$$

it is convenient to adopt Dirac's representation of the γ matrices. Let σ_i and ρ_i be two commuting sets of the standard (space-independent) Pauli matrices satisfying

$$\begin{aligned} \{\sigma_i, \sigma_j\} &= \{\rho_i, \rho_j\} = 2\delta_{ij}, \\ [\sigma_i, \rho_j] &= 0, \quad [\sigma_i, \sigma_j] = 2i\epsilon_{ijk} \sigma_k, \\ [\rho_i, \rho_j] &= 2i\epsilon_{ijk} \rho_k, \end{aligned} \quad (\text{A11})$$

where the roman indices vary from 1 to 3 (i.e., x to z). Choose the γ_μ and γ^μ matrices to be

$$\begin{aligned} \gamma^t &= -ie^{-u} \rho_3, \quad \gamma^i = e^{-v} \rho_2 \sigma_i, \\ \gamma_r &= ie^u \rho_3, \quad \gamma_i = e^v \rho_2 \sigma_i. \end{aligned} \quad (\text{A12})$$

It can be readily verified that

$$\Gamma_t = \frac{1}{2} \rho_1 \boldsymbol{\sigma} \cdot \mathbf{r} \frac{u'}{r} e^{u-v} \quad (\text{A13})$$

and

$$\boldsymbol{\Gamma} = -\frac{i}{2} (\boldsymbol{\sigma} \times \mathbf{r}) \frac{v'}{r},$$

where $u' = du/dr$, $v' = dv/dr$, and boldface denotes three-vectors. Consequently,

$$\Gamma_\mu \gamma^\mu + \gamma^\mu \Gamma_\mu = 0, \quad (\text{A14})$$

and (A5) becomes

$$\mathcal{L}(f) = \frac{1}{2} \left[\frac{\partial \bar{\psi}}{\partial x^\mu} \gamma^\mu \psi - \bar{\psi} \gamma^\mu \frac{\partial \psi}{\partial x^\mu} \right] - (m - f\sigma) \bar{\psi} \psi, \quad (\text{A15})$$

where for the explicit representation (A12), $\bar{\psi}$ is related to the Hermitian conjugate ψ^\dagger by

$$\bar{\psi} = \psi^\dagger \rho_3. \quad (\text{A16})$$

The corresponding Lagrangian is

$$L(f) \equiv \int e^{u+3v} \mathcal{L}(f) d^3r, \quad (\text{A17})$$

where $d^3r = dx dy dz$. By partial integration, $L(f)$ can also be written as

$$L(f) = - \int e^{u+3v} \bar{\psi} \left[\gamma^\mu \left[\frac{\partial}{\partial x^\mu} + \Gamma_\mu \right] \psi + (m - f\sigma) \psi \right] d^3r \quad (\text{A18})$$

in which the Γ_μ matrices reappear, in contrast with (A15).

2. Quantization

From (A18), it follows that

$$\frac{\partial L(f)}{\partial(\partial\psi/\partial t)} = ie^{3v} \psi^\dagger,$$

which leads to the quantization condition:

$$\{\psi(\mathbf{r}, t), \psi^\dagger(\mathbf{r}', t)\} = e^{-3v} \delta^3(\mathbf{r} - \mathbf{r}'). \quad (\text{A19})$$

Introduce

$$\chi \equiv \psi e^{3v/2}, \quad (\text{A20})$$

so that χ and χ^\dagger satisfy the canonical anticommutation relation

$$\{\chi(\mathbf{r}, t), \chi^\dagger(\mathbf{r}', t)\} = \delta^3(\mathbf{r} - \mathbf{r}'). \quad (\text{A21})$$

In terms of χ and χ^\dagger the Lagrangian $L(f)$ becomes

$$L(f) = \int d^3r \left[i \chi^\dagger \frac{\partial \chi}{\partial t} + ie^{(u-v)/2} \chi^\dagger \rho_1 \boldsymbol{\sigma} \cdot \nabla (e^{(u-v)/2} \chi) - e^u \rho_3 \chi^\dagger (m - f\sigma) \chi \right]. \quad (\text{A22})$$

Correspondingly, the fermion Hamiltonian is

$$H(f) = \int d^3r e^{(u-v)/2} \chi^\dagger [-i \rho_1 \boldsymbol{\sigma} \cdot \nabla + e^v \rho_3 (m - f\sigma)] \times e^{(u-v)/2} \chi. \quad (\text{A23})$$

The time component of j^μ is

$$j^t = \psi^\dagger \psi e^{-u} = \chi^\dagger \chi e^{-u-3v};$$

therefore, the fermion number

$$N \equiv \int j^t |g|^{1/2} d^3r = \int \chi^\dagger \chi d^3r. \quad (\text{A24})$$

3. Thomas-Fermi approximation

We assume that u , v , and σ are slowly varying functions. Divide the entire three-space into small cubes, labeled $n=1, 2, \dots$. The dimensions of these cubes are much larger than the de Broglie wavelength of the typical fermions in the system, yet sufficiently small that within each cube u , v , and σ can be approximated as constants.

Hence, we can write the operators $H(f)$ and N as sums over these cubes:

$$H(f) = \sum_n H_n(f) \quad (A25)$$

and

$$N = \sum_n N_n ,$$

where

$$\begin{aligned} H_n(f) &= e^{u(n)-v(n)} \int_n d^3r \chi^\dagger (-i\rho_1 \sigma \cdot \nabla + \rho_3 m_n) \chi , \\ N_n &= \int_n d^3r \chi^\dagger \chi , \\ m_n &= e^{v(n)} [m - f\sigma(n)] , \end{aligned} \quad (A26)$$

with the integral $\int_n d^3r$ extending only over the n th cube, and $u(n)$, $v(n)$, and $\sigma(n)$ the values of u , v , and σ within the cube. Inside that cube, we assume a degenerate Fermi distribution of free particles with a top momentum $p_F(n)$. The expectation values of $H_n(f)$ and N_n are given by

$$\langle H_n(f) \rangle = \frac{2}{8\pi^3} \int d^3p e^{u(n)-v(n)} n_p (p^2 + m_n^2)^{1/2} \quad (A27)$$

and

$$\langle N_n \rangle = \frac{2}{8\pi^3} \int d^3p n_p ,$$

where

$$n_p = \theta(p - p_F(n)) = \begin{cases} 0 & \text{if } p > p_F(n) , \\ 1 & \text{if } p < p_F(n) . \end{cases} \quad (A28)$$

Substituting these expressions into the expectation values of (A25), and returning the sum into integrals, we derive

$$\langle H(f) \rangle = \frac{2}{8\pi^3} \int d^3r \int d^3p n_p e^{u-v} [p^2 + e^{2v}(m - f\sigma)^2]^{1/2} \quad (A29)$$

and

$$\langle N \rangle = \frac{2}{8\pi^3} \int d^3r \int d^3p n_p$$

where, as in (A28),

$$n_p = \theta(p - p_F) . \quad (A30)$$

Note that in (A28), p refers to the fermion momentum in the laboratory frame; it is more convenient to use the corresponding momentum k in the local frame. Define

$$k = e^{-v} p , \quad (A31)$$

$$k_F = e^{-v} p_F ,$$

and

$$n_k = \theta(k - k_F) . \quad (A32)$$

We find

$$\langle H(f) \rangle = \frac{2}{8\pi^3} \int e^{u+3v} d^3r \int [k^2 + (m - f\sigma)^2]^{1/2} n_k d^3k$$

and

$$\langle N \rangle = \frac{2}{8\pi^3} \int e^{3v} d^3r \int n_k d^3k . \quad (A33)$$

Equations (2.16) and (2.17) are then derived; from these expressions all other Thomas-Fermi formulas used in Secs. II A and II B follow.

¹T. D. Lee, paper I, Phys. Rev. D **35**, 3637 (1987).

²R. Friedberg, T. D. Lee, and Y. Pang, paper II, Phys. Rev. D **35**, 3640 (1987).

³R. Friedberg, T. D. Lee, and Y. Pang, preceding paper, Phys. Rev. D **35**, 3658 (1987), hereafter referred to as III.

⁴R. Friedberg, T. D. Lee, and A. Sirlin, Phys. Rev. D **13**, 2739 (1976); Nucl. Phys. **B115**, 1 (1976); **B115**, 32 (1976).

⁵T. D. Lee, *Particle Physics and Introduction to Field Theory* (Harwood Academic, New York, 1981), Chap. 7.

⁶T. D. Lee and G. C. Wick, Phys. Rev. D **9**, 2291 (1974).

⁷A. Chodos, R. J. Jaffe, K. Johnson, C. B. Thorn, and V. F.

Weisskopf, Phys. Rev. D **9**, 3471 (1974); W. A. Bardeen, M. S. Chanowitz, S. D. Drell, M. Weinstein, and T. M. Yan, *ibid.* **11**, 1094 (1975).

⁸R. Friedberg and T. D. Lee, Phys. Rev. D **15**, 1694 (1977); **16**, 1096 (1977).

⁹T. D. Lee, Phys. Rev. D **8**, 1226 (1973); Phys. Rep. **9C**, 143 (1974).

¹⁰S. Weinberg, Phys. Rev. Lett. **37**, 657 (1976).

¹¹R. Arnowitt, S. Deser, and C. W. Misner, in *Gravitation: An Introduction to Current Research*, edited by L. Witten (Wiley-Interscience, New York, 1962), p. 227.